Journal of Fluorine Chemistry 135 (2012) 231–239

Contents lists available at SciVerse ScienceDirect

Journal of Fluorine Chemistry

journal homepage: www.elsevier.com/locate/fluor

Specific interaction modes in the crystal structures of oligofluorinated tolanes featuring additional electron donor and acceptor groups

Mario Stein [a], Ricarda Berger [a], Wilhelm Seichter [b], Jürg Hulliger [a], Edwin Weber [b,*]

[a] Department of Chemistry and Biochemistry, University of Berne, Freiestrasse 3, CH-3012 Berne, Switzerland
[b] Institute of Organic Chemistry, Technische Universität Bergakademie Freiberg, Leipziger Straße 29, D-09596 Freiberg, Sachsen, Germany

ARTICLE INFO

Article history:
Received 28 July 2011
Received in revised form 15 November 2011
Accepted 16 November 2011
Available online 25 November 2011

Keywords:
Substituted fluorotolanes
Sonogashira cross-coupling reaction
X-ray crystal structures
Supramolecular interactions
Fluorine involved contacts

ABSTRACT

A series of partially fluorinated and specifically *para*-substituted tolanes (**1**–**4**) have been synthesized via palladium-catalyzed Sonogashira cross-coupling reaction. The single-crystal structures have been determined by X-ray diffraction. The molecules adopt a geometry being more or less disturbed from planarity due to crystal packing effects. The packing structures are characterized by the formation of molecular stacks achieved through different modes of $\pi\cdots\pi$ interaction and being accomplished by other types of weak interactions including hydrogen bonds as well as bromo and in particular fluoro involved contacts.

© 2011 Elsevier B.V. All rights reserved.

1. Introduction

Compounds showing a simple basic structure with clear molecular geometry and having well defined substituents and functional groups are most desirable testing systems in order to increase the knowledge on non-covalent intermolecular interactions [1,2]. Corresponding weak intermolecular contacts are a fundamental tool in the field of crystal engineering, aiming at the control of a crystal structure from molecular construction [3,4]. This is of paramount importance in organic materials science since macroscopic properties of a solid such as electric and optical behaviour [5,6] as well as structural polymorphism [7] and catalysis [8], having widespread commercial implications, can be selectively influenced this way. In the course of these studies, different packing motifs in crystals including strong and weaker hydrogen bonding [9,10] or π-stacking interactions [11], giving rise to the formation of specific supramolecular synthons [1,12], have been discussed in detail. Making a more profound understanding of the nature and strength of organic halogen promoted non-covalent interactions [13] accessible, especially involving organic bound fluorine atoms in competition with other weak contacts [2,14], is another current challenge [15]. A motive for it is that fluorinated organic compounds often show uncommon and unique physical and chemical properties [16]. With relevance to molecules intended for the formation of metal–ligand network structures [17], liquid crystal behaviour [18] or crystals suitable for non-linear optical properties like second harmonic generation (SHG) [19], fluorination has been considered to control the strength of neighbouring donor and acceptor groups and thus affect their behaviour of supramolecular interaction. In this connection, partially fluorinated tolanes [20] and hetero derivatives of tolanes [21] have recently been synthesized and studied with reference to their crystalline packing structures.

Herein we report the synthesis of a series of similarly fluorinated tolanes **1**–**4** (Scheme 1) featuring, however, selected donor and acceptor groups in the *para* positions of the aryl rings and discuss their crystal structures in the light of the consequences coming from the fluorine substitution.

2. Results and discussion

2.1. Compounds studied

All the compounds **1**–**4** being substituted derivatives of tolane were synthesized following a common protocol in the key preparation step. This involves a Sonogashira–Hagihara cross-coupling reaction between a halogenated arene and an aryl substituted ethyne in the presence of a standard palladium(II)/copper(I) catalytic system [22]. The respective aryl halides (**5a**, **5b**) and corresponding arylethynes (**6a**–**6c**) are specified in Scheme 2. A complete synthetic route, exemplary shown for the preparation

---

* Corresponding author.
E-mail address: Edwin.Weber@chemie.tu-freiberg.de (E. Weber).

0022-1139/$ – see front matter © 2011 Elsevier B.V. All rights reserved.
doi:10.1016/j.jfluchem.2011.11.009

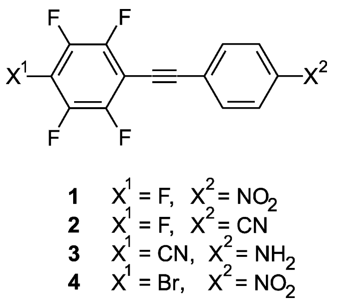

Scheme 1. Formula structures of compounds studied.

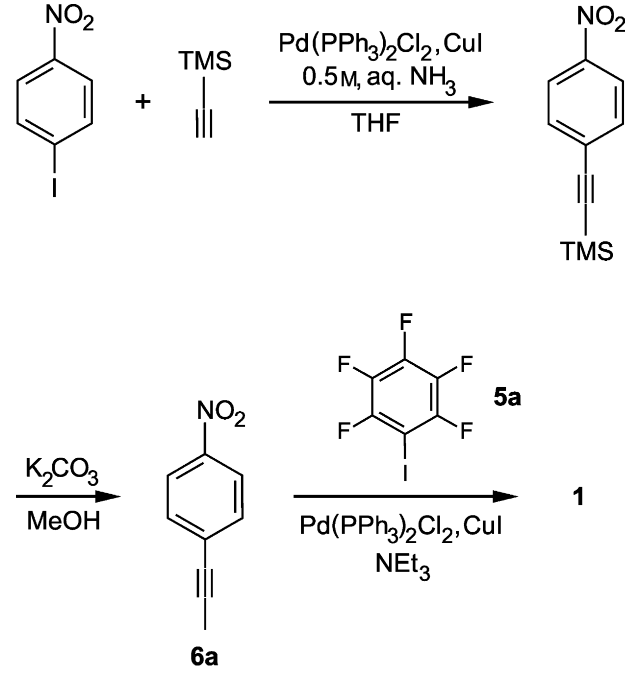

Scheme 3. Synthetic route exemplary demonstrated for compound **1**.

of compound **1**, is detailed in Scheme 3. Single crystals of the compounds **1**–**4** were obtained by slow evaporation of solutions of **1** and **4** in acetone, **2** in chloroform and **3** in dimethylsulfoxide.

2.2. X-ray single crystal structures

The crystallographic data and structure refinement parameters for the studied compounds (**1**–**4**) are summarized in Table 1. For the description of the crystal structures, intermolecular contacts within the sum of the van der Waals radii [23] have been used. Corresponding hydrogen bond type interactions (C–H···O, C–H···N, C–H···F, N–H···N) as well as C–F···π, N–O···O, N–O···N, Br···O and F···F contacts are presented in Table 2.

2.2.1. Nitropentafluoro-substituted tolane 1

Crystallization of **1** from acetone yielded yellow plates of the monoclinic space group $P2_1/c$ with one molecule in the asymmetric unit of the cell. The molecule (Fig. 1(a)) deviates from planarity and adopts a dihedral angle of nearly 9.9° between the mean planes of the aromatic rings. The nitro substituent is slightly tilted (ca. 2.5°) with respect to the aromatic ring to which it is attached.

In the crystal structure, the molecules are stacked along the *b*-axis in a head-to-head fashion. Within a given stack, consecutive molecules are strictly parallel but displaced by 3.64 Å in direction of their longitudinal axes. In this arrangement, the ethynyl moiety of each molecule is sandwiched in a distance of 3.50 Å between the perfluorophenyl and nitrophenyl rings of two neighbouring molecules which suggests the presence of $\pi_{(C\equiv C)}\cdots\pi_{(arene)}$ interactions [20,21] (Fig. 2). These findings are consistent with a recently arisen theoretical interaction model based on molecular electrostatic potentials [24] which provides a new view for simple explanation of the packing behaviour of molecules in crystalline perfluoroarene–arene complexes [25,26]. In this model, the geometries of arene stacking are induced by local substituent effects with the proximal vertex of the other ring rather than being caused by traditional π-polarization or quadrupole interaction [27,28] that was already questioned before [29]. The electron-withdrawing nature of the ring substituents in **1** relieves electrostatic repulsion between the aryl π-clouds which in the present case produces a longitudinal displacement of neighbouring molecules. The molecular planes of adjacent stacks are oriented approximately orthogonal thus forming an overall herringbone pattern. There appears to be no significant non-covalent bonding based on fluorine interactions [15]. The shortest C–H···F contact [C(2)–H(2)···F(1) 2.68 Å, 142°] is beyond the sum of the van der Waals radii (2.67), whereas the F···F distance (2.94 Å) represents the van der Waals limit. This suggests that fluorine involved interactions hardly contribute to crystal stabilization of **1**. However, an unusual feature of the crystal structure is the short distance between the nitro substituents of two adjacent molecules in the structure, showing O···O separations of 2.82 and 2.91 Å, which is less than twice the van der Waals radius of oxygen (3.04 Å). The structure excerpt displayed in Fig. 3 shows the contact mode between the nitro substituents. Due to the orthogonal orientation of the interacting molecules *I* and *II*, their nitro substituents approach each other in a perpendicular fashion with N–O···O and N–O···N angles (symmetry: $-x$, $0.5 + y$, $0.5 - z$) being 136.1 and 113.4°, respectively. The N–O···O angle between the symmetry related molecules *I* and *III* which adopt a coplanar arrangement (symmetry: $-x$, $1 - y$, $1 + z$) is 131.3°. In this context, it should be noted that similar close O···O contacts have also been observed in the crystal structures of a picric acid complex [30] and of 2,4,6-trinitrotoluene [31].

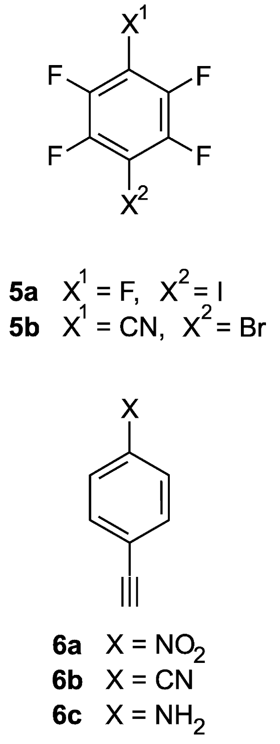

Scheme 2. Formula structures of fluoroarene and ethynylarene intermediates.

Table 1
Crystallographic and structure refinement data of the compounds studied.

Compound	**1**	**2**	**3**	**4**
Empirical formula	$C_{14}H_4F_5NO_2$	$C_{154}H_4F_5N$	$C_{15}H_6F_4N_2$	$C_{14}H_4F_4Br_1NO_2$
Formula weight	313.18	293.19	290.22	374.09
Crystal system	Monoclinic	Monoclinic	Triclinic	Triclinic
Space group	$P2_1/c$	$P2_1/c$	$P2_1/n$	P-1
a (Å)	20.003(4)	13.2995(10)	7.8158(17)	8.5057(13)
b (Å)	5.0291(6)	9.623(1)	5.8014(8)	8.7859(12)
c (Å)	12.107(2)	19.7667(15)	27.052(6)	9.1781(13)
α (°)	90.0	90.0	90.0	91.380(12)
β (°)	90.391(15)	106.393(6)	97.204(18)	102.526(12)
γ (°)	90.0	90.0	90.0	92.975(11)
V (Å^3)	1217.9(3)	2426.9(4)	1216.9(4)	668.21(17)
Z	4	8	4	2
$F(000)$	624	1168	584	364
D_c (mg m^{-3})	1.708	1.605	1.584	1.859
μ (mm^{-1})	0.166	0.149	0.139	3.129
Data collection				
Temperature (K)	223(2)	223(2)	173(2)	223(2)
No. of collected reflections	9184	34137	7669	9734
Within the θ-limit (°)	2.0–25.7	1.6–29.3	1.5–25.7	2.3–29.3
Index ranges $\pm h$, $\pm k$, $\pm l$	−24/24, −6/6, −14/14	−18/18, −13/13, −23/27	−9/9, −7/6, −32/32	−11/11, −12/10, −12/12
No. of unique reflections	2289	6566	2293	3610
R_{int}	0.0629	0.0600	0.0659	0.0601
Refinement calculations: full-matrix least-squares on all F^2 values				
Weighting expression w[a]	$[\sigma^2(F_o^2)+(0.0367P)^2$ $+ (0.0000P)^{-1}]$	$[\sigma^2(F_o^2)+(0.0551P)^2$ $+(0.0000P)^{-1}]$	$[\sigma^2(F_o^2)+(0.0287P)^2$ $+(0.0000P)^{-1}]$	$[\sigma^2(F_o^2)+(0.0940P)^2$ $+(0.0000P)^{-1}]$
No. of refined parameters	200	380	215	199
No. of F values used $[I>2\sigma(I)]$	1290	3251	1182	2036
Final R-indices				
$R(=\Sigma\|\Delta F\|/\Sigma\|F_o\|)$	0.0385	0.0390	0.0382	0.0592
wR on F^2	0.0827	0.1093	0.0744	0.1644
S (=goodness of fit on F^2)	0.873	0.862	0.787	0.961
Final $\Delta\rho_{max}/\Delta\rho_{min}$ (e Å^{-3})	0.15/−0.13	0.23/−0.16	0.19/−0.22	0.91/−0.99

[a] $P=(F_o^2+2F_c^2)/3$.

Table 2
Selected hydrogen bond and other non-covalent interactions in the compounds **1**–**4**.

Atoms involved	Symmetry	Distances (Å)			Angles (°)
		D–H X–Y (X = C,N; Y = O,F, Br)	D···A Y···A	H···A X···A	D-H···A X-Y···A (A = N, O, F, π)
1					
C(6)–H(6)···O(1)	x, −0.5−y, 0.5 + z	0.94	3.354(2)	2.72	125
C(5)–H(5)···O(2)	−x, −1 − y, 1 − z	0.94	3.504(2)	2.67	149
C(2)–H(2)···F(1)	x, 1.5 − y, −0.5 + z	0.94	3.470(2)	2.68	142
N(1)–O(1)···O(2)	−x, −0.5 + y, 0.5 − z	1.22	3.887(2)	2.91	136.1
N(1)–O(1)···N(1)	−x, −0.5 + y, 0.5 − z	1.22	3.573(2)	2.91	113.4
N(1)–O(2)···O(2)	−x, −1 − y, 1 − z	1.22	3.740(2)	2.83	131.3
C(14)–F(5)···F(2)	x, 1.5 − y, −0.5 + z	1.34	4.140(2)	2.94	147.9
C(11)–F(2)···F(5)	x, 1.5 − y, 0.5 + z	1.34	3.168(2)	2.94	87.0
2					
C(5A)–H(5A)···N(1)	x, 0.5 − y, −0.5 + z	0.94	3.591(2)	2.66	170
C(3)–H(3)···N(1A)	x, 0.5 − y, 0.5 + z	0.94	3.533(2)	2.60	171
C(5)–H(5)···F(5A)	−1 + x, y, z	0.94	3.258(2)	2.66	122
C(13)–F(4)···*centroid*(A′)[a]	1 − x, 2 − y, 0.5 − z	1.34	4.345(2)	3.04	163.7
C(11A)–F(2A) ·*centroid*(A′)[a]	1 − x, 0.5 + y, 0.5 − z	1.33	4.351(2)	3.05	167.4
3					
C(6)–H(6)···F(1)	1 − x, 1 − y, −z	0.93	3.568(2)	2.74	149
C(3)–H(3)···F(3)	−x, −1 − y, −z	1.00	3.357(2)	2.61	132
N(1)–H(1B)···N(1)	0.5 − x, 0.5 + y, 0.5 − z	0.91	3.452(2)	2.64	149
N(1)–H(1A)···N(2)	−0.5 + x, −0.5 − y, 0.5 + z	0.91	3.265(2)	2.43	153
C(3)–H(3)···N(2)	−0.5 + x, −0.5 − y, 0.5 + z	1.00	3.468(2)	2.64	140
C(10)–F(1)···F(3)	x, 1 + y, z	1.35	3.023(2)	2.88	82.8
C(13)–F(3)···F(1)	x, −1 + y, z	1.34	3.014(2)	2.88	82.5
4					
C(3)–H(3)···O(1)	−x, 1 − y, 1 − z	0.94	3.424(2)	2.63	142
C(5)–H(5)···O(2)	1 − x, 1 − y, 2 − z	0.94	3.469(2)	2.70	140
C(3)–H(3)···F(1)	−1 + x, y, z	0.94	3.102(2)	2.63	111
C(5)–H(5)···F(3)	x, 1 + y, 1 + z	0.94	3.472(2)	2.68	143
C(12)–Br(1)···O(1)	1 − x, −1 + y, −1 + z	1.86	4.988(2)	3.19	161.6
C(12)–Br(1)···O(2)	1 − x, −1 + y, −1 + z	1.86	4.963(2)	3.19	157.7
C(14)–F(4)···F(4)	1 − x, −y, −z	1.40	3.017(2)	2.91	80.3

[a] Means the center of the triple bond [C(7)–C(8)].

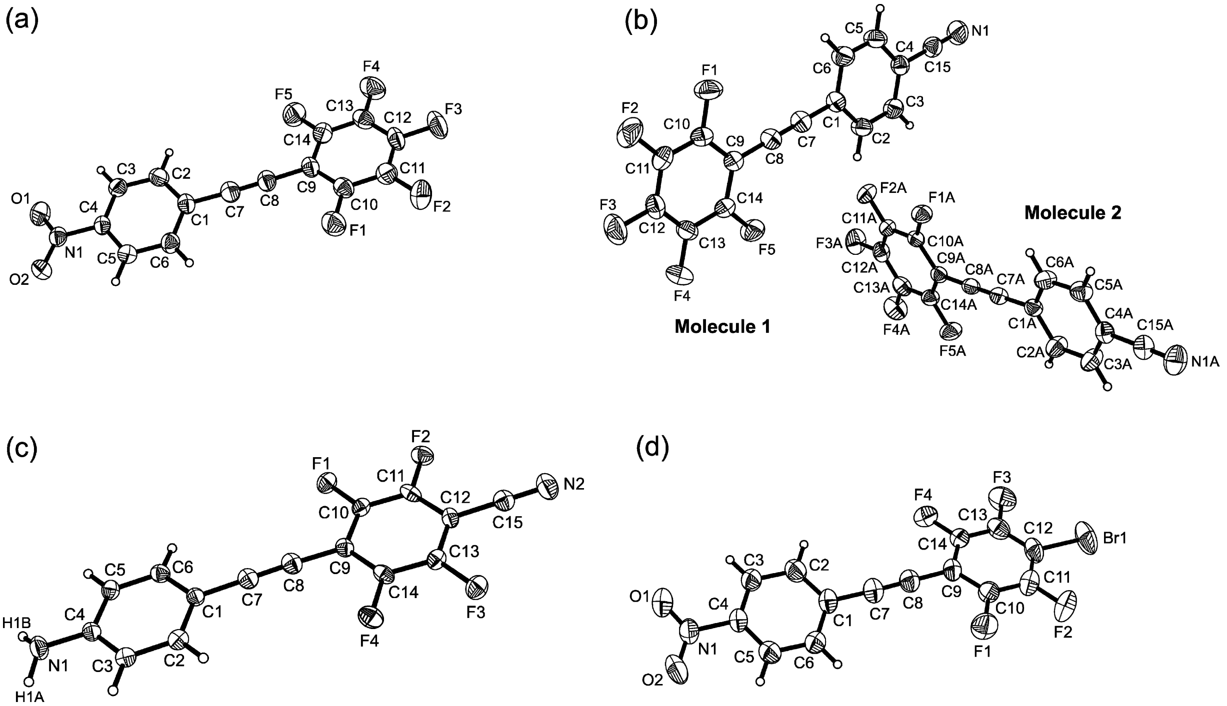

Fig. 1. ORTEP plots of the molecular structures of compounds **1**–**4** including atom labelling. Thermal ellipsoids are drawn at 50% probability level.

2.2.2. Cyanopentafluoro-substituted tolane **2**

Crystallization of **2** from chloroform yielded colourless crystals of the monoclinic space group $P2_1/c$ with two crystallographically independent molecules within the asymmetric part of the unit cell. A perspective view of the molecular structure is depicted in Fig. 1(b). The molecules are approximately planar with a dihedral angle of 3.0° between the aromatic moieties.

The basic supramolecular units of the crystal structure are given by C–H···N bonded molecular dimers [d(H···N) 2.60, 2.66 Å], which are assembled to stacking-like structure domains (Fig. 4) extending parallel to the crystallographic 1 0 1 plane. Within this arrangement, the stacking order of molecules can be described as AABBAA..., which means that every fourth molecule along the stacking axis is congruent. Also in the crystal of **2** the lack of arene

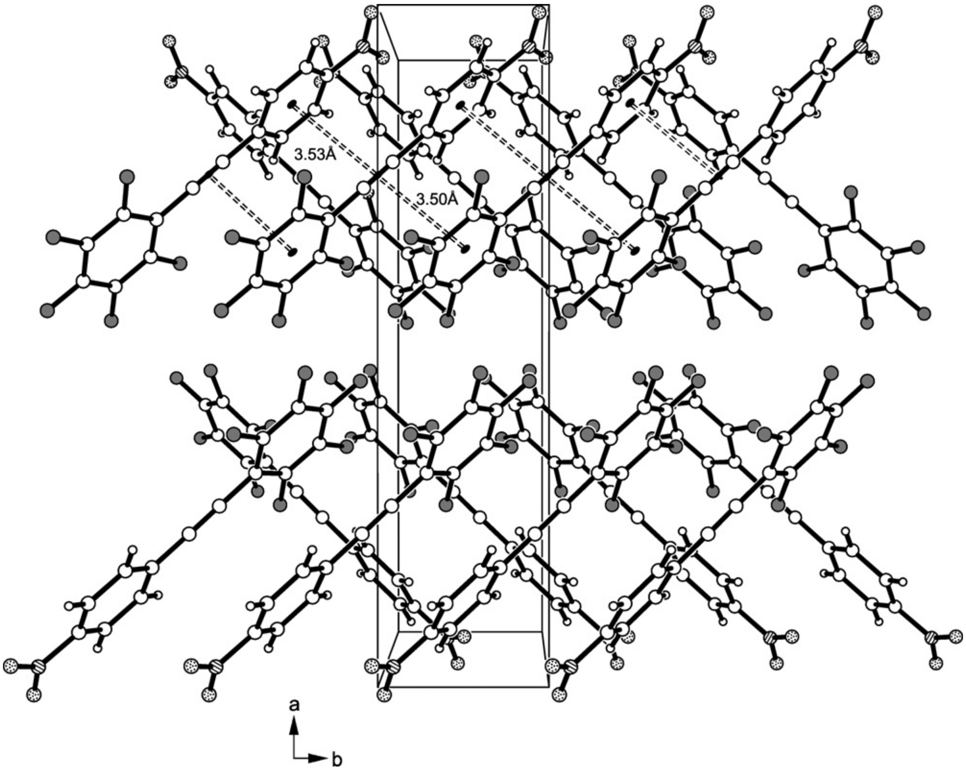

Fig. 2. Packing diagram of **1** viewed down the crystallographic c-axis. Oxygen atoms are displayed as dotted, nitrogen atoms as hatched and fluorine atoms as dark grey circles. Broken double lines represent π(ethynyl)···π(arene) interactions.

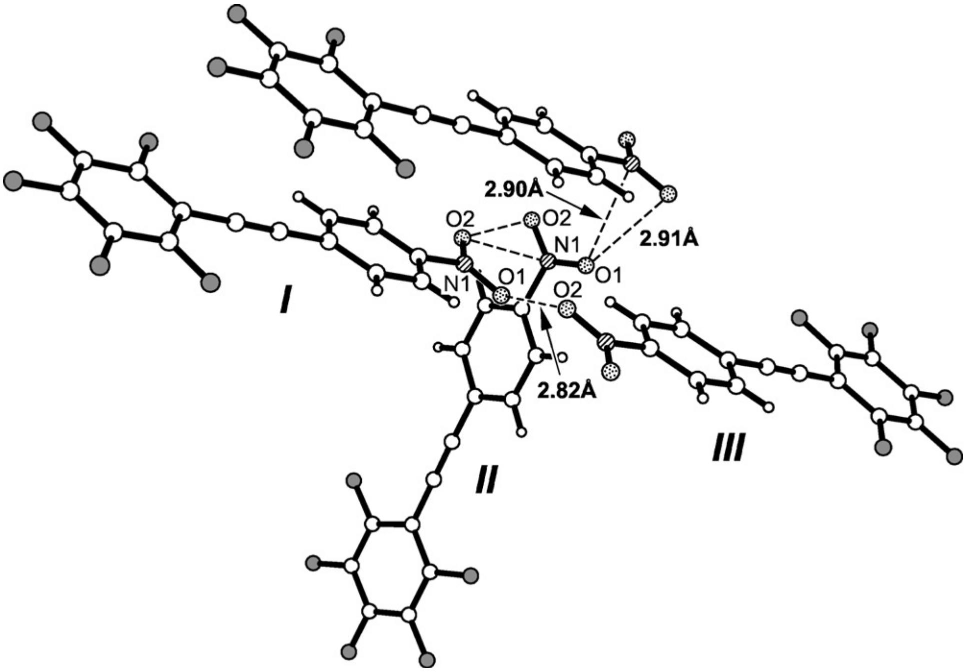

Fig. 3. Packing excerpt of **1** showing the mode of interactions between the nitro substituents of the molecules. Oxygen atoms are displayed as dotted, nitrogen atoms as hatched and fluorine atoms as dark grey circles. Broken lines represent O···O and O···N contacts.

stacking is attributable to the electron-withdrawing character of the arene substituents which depletes the π-electron density of both aromatic rings. In this structure, the hydrogen bonded ring motifs of the dimers are located between the perfluorophenyl and benzonitrile part of neighbouring molecules. In a similar fashion as in the aforementioned crystal structure, molecular planes of adjacent stacks are nearly perpendicular. Interstack association is restricted to weak C–H···F contacts [C(5)–H(5)···F(5A) 2.66 Å, 122°] and C–F···(C≡C) interactions involving the fluorine atoms F(4) and F(2A) and the central ethynyl unit of the molecule 2. With reference to the latter interactions, both the F···*centroid*(C≡C) distances of 3.04 (3.05) Å, being less than the sum of van der Waals radii (3.17 Å), and the well defined geometry of this contacts (∠C–F···*centroid* 163.7, 167.4°), demonstrate evidence of fluorine-centered bonding based on the σ-hole approach [32].

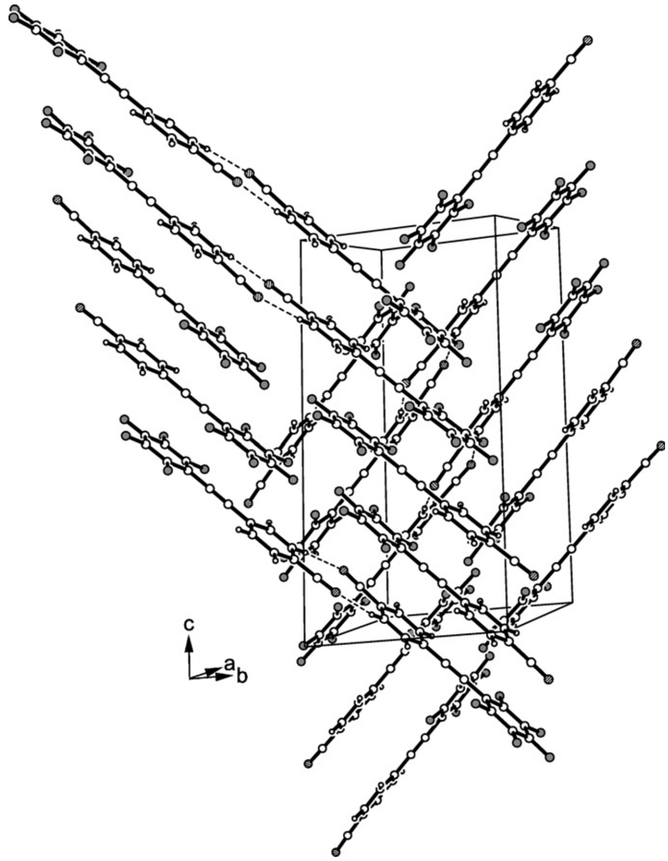

Fig. 4. Packing diagram of **2**. Nitrogen atoms are displayed as hatched and fluorine atoms as dark grey circles. Broken double lines represent C–H···N hydrogen bonds.

2.2.3. Aminocyanotetrafluoro-substituted tolane 3

Crystal growing of **3** from a solution in DMSO yielded yellow plates which show the monoclinic space group $P2_1/n$ with the asymmetric unit cell containing one molecule. A perspective view of the molecular structure is presented in Fig. 1(c). From the structural viewpoint, donor–acceptor functionalized diaryl acetylenes should be characterized by a redistribution of charge from donor to acceptor across the conjugated π-electron system, giving rise to ground-state charge-transfer activity [33]. As a matter of fact, a detailed analysis of the molecular structure of **3** reveals only a small partial quinoid character of the tetrafluorobenzonitrile part, which is obvious from bond distances within the aromatic ring ranging from 1.360(3) to 1.396(4) Å. In contrast, the aminophenyl donor group is far from being planar, but the plane of the amino substituent is inclined at an angle of nearly 30° with regard to the phenyl ring plane. This can be seen as an indication for the difference in conjugation of the two aromatic entities, while the bridging ethynyl unit possesses a distinctive single bond–triple bond alternation pattern. Nevertheless, our findings are consistent with the structures of a previously studied series of donor–acceptor (amino–nitro) *para*-substituted diarylalkynes [34].

In the crystal structure of **3** (Fig. 5), the molecules are stacked in direction of the crystallographic *a*-axis with an antiparallel arrangement of consecutive molecules. The *centroid*···*centroid* distances between the aromatic rings of interacting molecules are 3.78 (symmetry: $-x, -y, -z$) and 4.11 Å (symmetry: $1-x, -y, -z$).

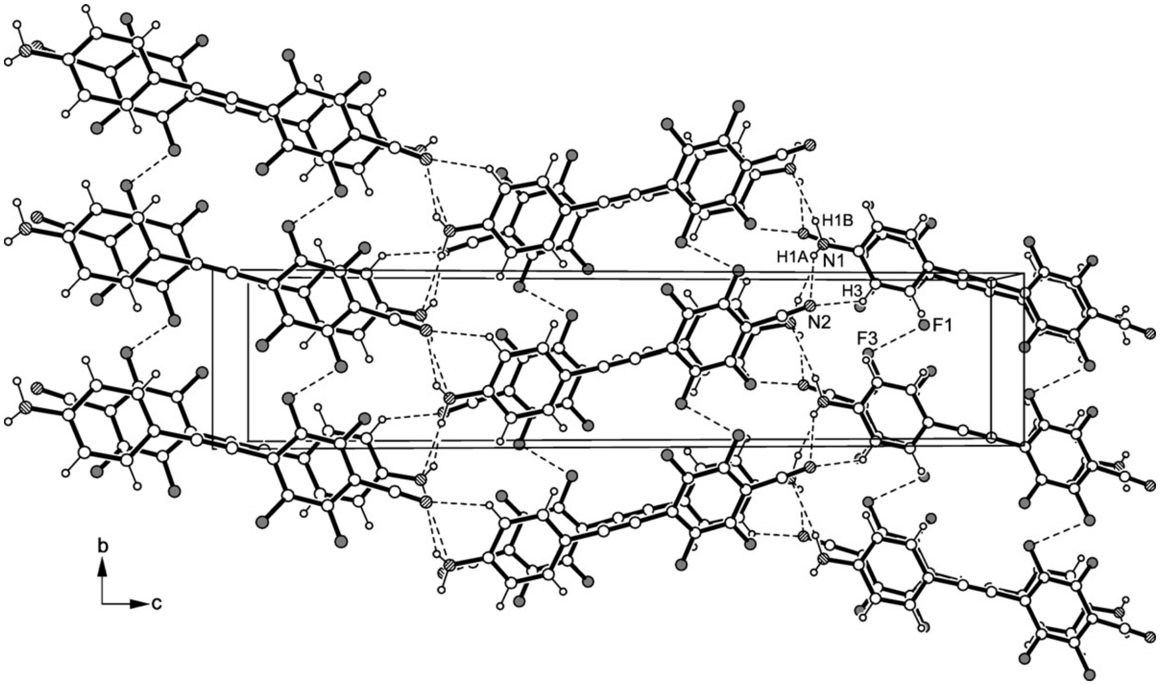

Fig. 5. Packing diagram of **3** viewed down the crystallographic *a*-axis. Nitrogen atoms are displayed as hatched and fluorine atoms as dark grey circles. Broken lines represent hydrogen bonds and F···F contacts.

Due to the above mentioned theoretical interaction model [24], the donor–acceptor character of the substituents in **3** implies electrostatic potential values of opposite signs for the aromatic molecular building blocks which should lead to a electrostatic attraction between dissimilar arene rings of consecutive molecules. However, strong directional interactions induce a molecular offset within the stacking arrangement which significantly reduces the effective overlapping area between aromatic units and thus diminishes the strength of stacking forces. The well-balanced ratio between strong molecular donors and acceptors induces a tight network of hydrogen bonds. The molecular stacks are interlinked via N–H···$N_{(amine)}$ [N(1)–H(1B)···N(1) 2.64 Å, 140°] and N–H···$N_{(nitrile)}$ hydrogen bonds [N(1)–H(1A)···N(2) 2.43 Å, 153°] as well as weak F···F contacts [15] [F(1)···F(3) 2.88 Å]. Moreover, the

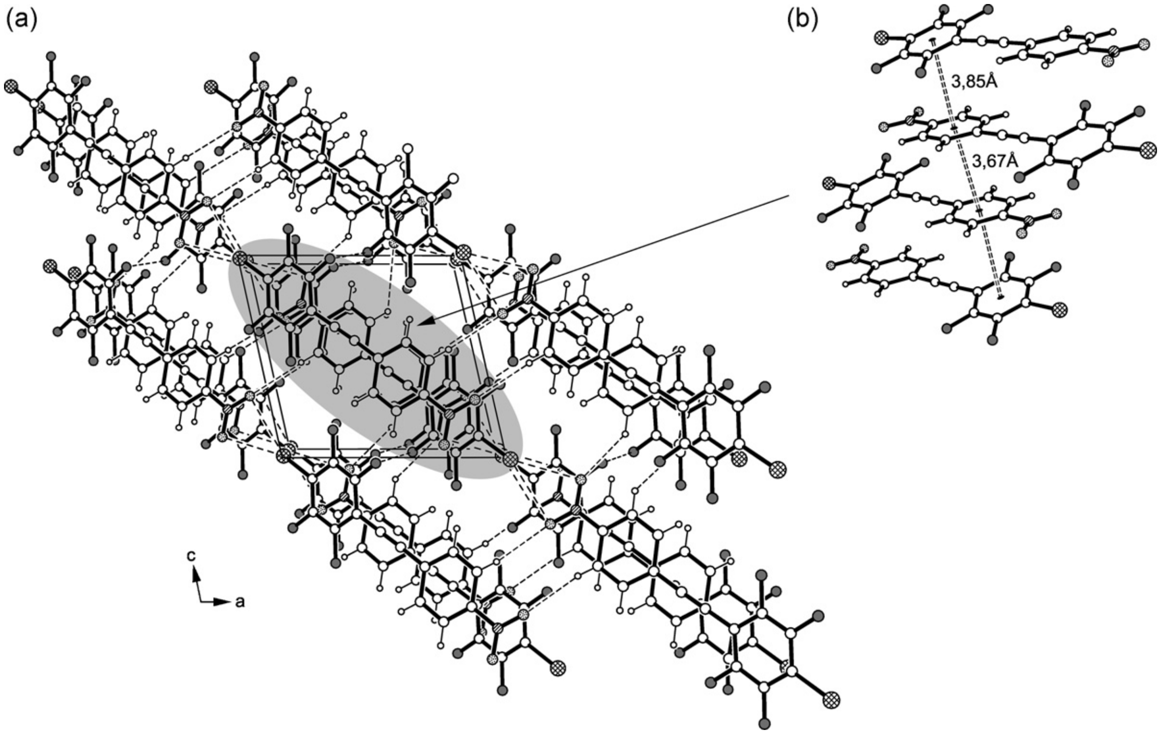

Fig. 6. (a) Packing diagram of **4** viewed down the crystallographic *b*-axis. Oxygen atoms are displayed as dotted, nitrogen atoms as hatched, bromine atoms as cross-hatched and fluorine atoms as dark grey circles. Broken lines represent hydrogen bonds and F···F contacts. (b) Mode of arene stacking.

nitrile nitrogen is involved in weak C–H···N interactions [9] [C(3)–H(3)···N(2) 2.64 Å, 140°].

2.2.4. Bromonitrotetrafluoro-substituted tolane 4

Crystallization of **4** from acetone yielded colourless plates of the space group *P*-1 (*Z* = 2). A perspective view of the molecule is shown in Fig. 1(d). The twist angle between the aromatic rings is about 15.0°, whereas the nitrophenyl moiety adopts a nearly planar conformation. The C–Br bond distance of 1.863(4) Å, which is less than the average value of bromophenyl derivatives (ca. 1.90 Å), indicates a partial double bond character, which may be ascribed to polarization effects of the fluorine atoms. As for **3**, the central ethynyl fragment shows alternating single bond–triple bond character.

The crystal structure of **4** (Fig. 6) is composed of linear supramolecular strands with the molecules being connected in a head-to-tail fashion via C–Br···O contacts. Geometric parameters [*d*(Br···O) 3.19, 3.19 Å; ∠C–Br···O 161.6, 157.7°] show these contacts as being typical of halogen bonds [35]. These chains are stacked along the crystallographic *b*-axis. Within the stacking structure, each phenyl ring is located between an equivalent ring and an unequivalent fluorinated ring with *centroid···centroid* distances of 3.67 (*phenyl···phenyl*) and 3.85 Å (*phenyl·····fluorophenyl*).Interstack association is accomplished by numerous weak interactions comprising C–H···O hydrogen bonds [9] [*d*(H···O) 2.63, 2.70 Å] and C–H···F [*d*(H···F) 2.63, 2.68 Å] as well as F···F contacts [*d*(F···F) 2.91 Å].

3. Conclusions

A comparative inspection of the crystal structures of the partially fluorinated and differently *para*-substituted tolanes **1**–**4** carried out in terms of a recent theoretical model based on molecular electrostatic potentials (ESPs) [24] reveals some interesting features as specified in the following.

Analogous to the solid phase structures of tolane [36] and its functionalized derivatives [3,5–7], the compounds **1**–**4** adopt a geometry which is more or less disturbed from planarity due to crystal packing effects. The tendency to form columnar packing structures is characteristic for this kind of compounds and resembles those found in a variety of 1:1 complexes of an aromatic hydrocarbon and a perfluoroarene component [25,26]. However, ideal alternate stacking is only realized in co-crystals with weak interstack association. In such systems, local substituent effects have been discussed as a driving force for the stacking formation.

In the molecular structures **1**–**4**, the presence of *para*-substituents at the phenyl part and the fluorinated ring in **3** and **4** affects the electrostatic potentials of the respective arene unit. The electron withdrawing character of the substituents in **1** induces repulsion between the π-clouds of dissimilar aromatic units. This property results in a considerable longitudinal offset of parallel molecules giving rise to $\pi_{(C\equiv C)}\cdots\pi_{(arene)}$ interactions. In principle, the crystal structure of the corresponding nitrile **2** shows a similar packing behaviour, but due to the lateral offset of neighbouring molecules, the stacking structure lacks π···π interactions. Instead, C–H···N bonds which link the molecules to dimers, as well as intermolecular contacts of the $C–F\cdots\pi_{(C\equiv C)}$ type, taking geometric parameters of the σ-hole concept into account [32] stabilize the crystal packing. The complementary character of the *para*-substituents of compound **3** induces a stacking arrangement with an antiparallel orientation of consecutive molecules, which is typical for the crystal structures of phenyl–fluorophenyl ethynes [18,20,37] and corresponding stilbenes [38]. Due to the donor/acceptor ability of **3**, the molecular stacks are interlinked by a tight network of non-covalent bonds including N–H···N and C–H···N type hydrogen bonds. In a similar fashion, the bromine atom in **4** acts as a halogen bonding donor site, leading to a crystal structure which is constructed of molecular C–Br···O bonded head-to-tail chains. They are further assembled to 2D stacking-like domains with an opposite running direction of neighbouring strands. The offset between molecules induces a stacking order of aromatic residues which is different from **3** and can be described as phenyl^F–(phenyl)$_2$–phenyl^F. In all cases, weak C–H···F and C–F···F contacts are likely to be present, the distances of which are near the van der Waals limit. Hence, it is questionable whether they are relevant for crystal structure stabilization of the compounds.

Another point worth mentioning is that the donor/acceptor character of **3** and **4** may give rise to a potential ground-state charge-transfer activity, which should be represented by a partial "quinoid" resonance structure of the molecules [33]. Surprisingly, the analysis of bond lengths around the central ethynyl fragment reveals that neither the fluorination nor the presence of *para*-substituents show any significant influence on the C(sp^2)–C(sp) and C(sp)–C(sp) bond distances since they were found in conformity with plain tolane [36]. This means that the ethynyl unit in **3** and **4** does not take part in perceptible charge-transfer [34].

In summary, it is illustrated that the tolanes **1**–**4**, although featuring rather similar conformational geometry of the basic molecular framework (only the compound **4** possesses moderate distortion of the aryl rings from coplanarity), show different packing structures determined both by the functional groups and the fluorine substitution but with an obvious preference to π-stacking interactions involving the fluorinated and non-fluorinated phenyl as well as the ethynyl moiety. This is a behaviour largely corresponding with previous studies [20,34], thus making a potential guiding principle for the purpose of crystal engineering such as the alignment of molecules required for a particular materials property.

4. Experimental

4.1. General

Melting points were determined using a microscope heating stage PHMK Rapido (VEB Wägetechnik) and are uncorrected. IR spectra were measured on FT-IR 510 Nicolet as KBr pellets. ^{1}H NMR and ^{13}C NMR spectra were obtained using a Bruker Avance 300 Spectrometer at 300 MHz (^{1}H) or 75 MHz (^{13}C); measurements were carried out at 25 °C with TMS as an internal standard. ^{19}F NMR spectra were recorded on Bruker DNRX 400 at 376 MHz with trichlorofluoromethane as external standard. Coupling constants are given in Hz and resonance multiplicities are described as s (singlet), d (doublet), t (triplet), m (multiplet). Assignment of the signals base on increment calculation [39]. Mass spectra (GC/MS) were determined with a Perkin Elmer SCIEX instrument. TLC was performed on aluminium plates coated with $SiO_2 60F_{254}$ (Merck). For column chromatography Merck silica gel 60 (0.063–0.1 mm) was used. Solvent for Sonogashira–Hagihara coupling reactions was deoxygenated prior to use by ultrasound (20 min) while bubbling argon through the solution.

The following compounds were prepared according to literature procedures: 4-bromo-2,3,5,6-tetrafluorobenzonitrile (**5a**) (from pentafluorobenzonitrile with lithium bromide) [40], 4-ethynylnitrobenzene (**6a**) [41] and 4-ethynylaniline (**6c**) [42] (from the respective *p*-substituted iodobenzenes and trimethylsilylacetylene followed by deprotection). 4-Iodonitrobenzene, 4-iodobenzonitrile, 4-iodoaniline as well as pentafluoroiodobenzene and bis(triphenylphosphane)palladium(II) chloride were purchased from commercial sources (Aldrich, Alfa, Aesar, Lancaster).

4.2. Syntheses of compounds 1–3

The respective halogenated oligofluorobenzene (2.0 mmol) and the corresponding terminal ethynyl compound (2.2 mmol) were dissolved in degassed triethylamine (20 ml). To this solution, the catalyst, being composed of bis(triphenylphosphane)palladium(II) chloride (22 mg, 0.03 mmol) and copper(I) iodide (5.6 mg, 0.03 mmol), was added and the mixture was stirred at 50 °C under argon for 16 h. The mixture was filtered through Celite, the filtration residue washed with diethyl ether and the combined organic layers evaporated. Column chromatography (SiO_2, eluent : hexane–ethyl acetate) yielded the pure compounds. Specific details for each compound are given below.

4.2.1. 4-[(Pentafluoropheny)ethyny]nitrobenzene (1)

Pentafluoroiodobenzene (**5a**) (0.59 g, 2.0 mm) and 4-(ethynyl)-nitrobenzene (**6a**) (0.33 g, 2.2 mmol) were used; ratio of the elution solvents hexane:ethyl acetate 10:1 (v/v). Yield 0.36 g (57%) yellow solid; mp: 162–164 °C, lit. [43] mp: 137–138 °C. IR (KBr): ν_{max} (cm^{-1}) 3104, 3085 (CH_{Ar}), 2223 (C≡C), 1595, 1522, 1501 ($C{=}C_{Ar}$), 1540, 1347 (NO_2), 1106 (C–F), 992, 967, 855 (CH_{Ar}, 1,4-disubst.). ^1H NMR ($CDCl_3$): δ_H 7.74 (d, $^3J_{HH}$ = 8.9 Hz, 2H, Ar–H), 8.27 (d, $^3J_{HH}$ = 10.23 Hz, 2H, Ar–H); ^{13}C NMR ($CDCl_3$): δ_C 77.8 ($C{\equiv}CAr^F$), 98.9 ($C{\equiv}CAr^H$), 99.3 (t, $^2J_{CF}$ = 18 Hz), Ar^F, 123.9 (Ar^H), 128.3 (Ar^H), 132.9 (Ar^H), 137.9 (d, $^1J_{CF}$ = −256 Hz, Ar^F), 142.3 (d, $^1J_{CF}$ = −257 Hz), 147.4 (d, $^1J_{CF}$ = 258 Hz), Ar^F, 148.1 (C–NO_2); ^{19}F NMR ($CDCL_3$); δ_F = −134.1 (d, $^3J_{FF}$ = 23 Hz), −150.6 (t, $^3J_{FF}$ = 21 Hz), −161.1 (t, $^3J_{FF}$ = 21 Hz). MS (GC/MS) m/z: 313 $[M]^+$.

4.2.2. 4-[(Pentafluorophenyl)ethynyl]benzonitrile (2)

Pentafluoroiodobenzene (**5a**) (0.59 g, 2.0 mmol) and 4-(ethynyl)nitrobenzene (0.25 g, 2.2 mmol) were used; ratio of the elution solvents hexane:ethyl acetate 3:1 (v/v). Yield 0.35 g (76%) colourless solid; mp: 163 °C. IR (KBr): ν_{max} (cm^{-1}) 3068 (CH_{Ar}), 2229 (C≡N), 1604,1523, 1499 ($C{=}C_{Ar}$), 1112 (C–F), 964, 843, 831 (CH_{Ar}, 1,4-disubst.). ^1H NMR ($COCl_3$): δ_H 7.67 (s, 2H, Ar–H), 7.67 (s, 2H, Ar–H); ^{13}C NMR ($CDCl_3$): δ_C 99.3 ($C{\equiv}CAr^F$), 99.32 ($C{\equiv}CAr^H$), 99.6 (t, $^2J_{CF}$ = 18 Hz, Ar^F), 11.2 (C–CN), 118.2 (C≡N), 1256.3 (Ar^H), 132.3 (Ar^H), 132.5 (Ar^H), 137.8 (d, $^1J_{CF}$ = −255 Hz, Ar^F), 142.2 (d, $^1J_{CF}$ = 257 Hz, Ar^F), 147.4 (d, $^1J_{CF}$ = −246 Hz, Ar^F); ^{19}F NMR ($CDCl_3$) δ_F −135.3 (d, $^3J_{FF}$ = 21 Hz), −150.8 (t, $^3J_{FF}$ = 21 Hz), −161.1 (t, $^3J_{FF}$ = 21 Hz). MS (GC/MS) m/z: 293 $[M]^+$.

4.2.3. 4-[(4-Aminophenyl)ethynyl]-2,3,5,6-tetrafluorobenzonitrile (3)

4-Bromo-2,3,5,6-tetrafluorobenzonitrile (0.51 g, 2.0 mmol) and 4-ethynylaniline (0.26 g, 2.2 mmol) were used. The reaction mixture was filtered and the residue was washed with acetone (2 × 10 mL), instead of diethyl ether; ratio of the elution solvents hexane:ethyl acetate 3:1 (v/v). Yield 0.11 g (19%) yellow solid; mp: 140 °C (dec.). IR (KBr): ν_{max} (cm^{-1}) 3451, 3360 (NH_2), 2213 (C≡N), 1649, 1622, 1596, 1518, 1488 ($C{=}C_{Ar}$), 1178 (C–F), 979, 835 (CH_{Ar}, 1,4-disubst.). ^1H NMR (DMSO-d_6): δ_H 6.01 (s, 2H, NH_2), 6.60 (d, $^3J_{HH}$ = 6.5 Hz, 2H, Ar–H), 7.29 (d, $^3J_{HH}$ = 6.5 Hz, 2H, Ar–H); ^{13}C NMR (DMSO-d_6): δ_C 72.4 (C–C≡N), 91.5 (Ar^H), 104.8 (C≡N), 108.3 ($C{\equiv}CAr^F$), 109.9 ($C{\equiv}CAr^H$), 110.9 (Ar^F), 113.6 (Ar^H), 133.7 (Ar^H), 145.3 (d, $^1J_{CF}$ = 186 Hz, Ar^F), 146.8 (d, $^1J_{CF}$ = 191 Hz, Ar^F), 151.7 (C–NH_2); ^{19}F NMR (DMSO-d_6): δ_F −134.8 (m), −136.8 (m). MS (GC/MS) m/z: 290 $[M]^+$.

4.3. Synthesis of 4-[(4-nitrophenyl)ethynyl]-2,3,5,6-tetrafluorobromobenzene (4)

A solution of 4-[(pentafluorophenyl)ethynyl]nitrobenzene (0.31 g, 1.0 mmol) and lithium bromide (8 mg, 1.0 mmol) in 1-methyl-2-pyrrolidon (3 mL) was stirred at 230 °C for 4.5 h. After cooling down to room temperature, the mixture was poured into water (10 mL). The precipitate which formed was collected, washed with water and dissolved in chloroform. The organic layer was washed with water and the aqueous phase extracted with chloroform. The combined organic phases were dried (Na_2SO_4) and evaporated under reduced pressure. Column chromatography (SiO_2, eluent: hexane–ethyl acetate, 3:1, v/v) led to the isolation of a small amount (≈1% yield) of the product as yellow solid. IR (KBr): ν_{max} (cm^{-1}) 3068 (CH_{Ar}), 2229 (C≡N), 1604, 1523, 1499 ($C{=}C_{Ar}$), 1112 (C–F), 964, 843, 831 (CH_{Ar}, 1,4-disubst.). ^1H NMR ($CDCl_3$): δ_H 7.75 (d, $^3J_{HH}$ = 8.9 Hz, 2H, Ar–H), 7.67 (s, 2H, Ar–H); ^{13}C NMR ($CDCl_3$): δ_C 78.8 ($C{\equiv}Car^F$), 99.8 (t, $^3J_{CF}$ = 18 Hz, Ar^F), 102.1 ($C{\equiv}Car^H$), 103.4 (C–Br), 123.9 (Ar^H), 128.2 (Ar^H), 132.9 (Ar^H), 145.0 (d, $^1J_{CF}$ = 245 Hz, Ar^F), 147.0 (d, $^1J_{CF}$ = 254 Hz, Ar^F), 148.1 (C–NO_2); ^{19}F NMR ($CDCl_3$): δ_F −134.4 (d, $^3J_{FF}$ = 19 Hz), −150.8 (d, $^3J_{FF}$ = 18 Hz). MS (GC/MS) m/z: 374 $[M]^+$.

4.4. X-ray structure determination

Crystals of **1**–**4** suitable for structure analysis were obtained by slow evaporation of solutions of the respective compounds in acetone (**1**, **4**), chloroform (**2**), and dimethylsulfoxide (**3**). The intensity data were collected on a Stoe Mark II-Image Plate diffractometer with MoK_α radiation (λ = 0.71073 Å). Reflections were corrected for background, Lorentz and polarization effects. Preliminary structure models were derived by application of direct methods [44] and were refined by full-matrix least squares calculation based on F^2 for all reflections [45]. With the exception of the hydrogens in **3**, all other hydrogen atoms were included in the models in calculated positions and were refined as constrained to bonding atoms.

All crystal data and experimental parameters are summarized in Table 1. Crystallographic data (excluding structure factors) for the structures in this paper have been deposited with the Cambridge Crystallographic Data Centre as supplementary publication nos. CCDC 818168–818171. Copies of the data can be obtained, free of charg on application to CCDC, 12 Union Road, Cambridge CB2 1EZ, UK (fax: +44 1223 336033 or deposit @ccde.cam.ac.uk).

Acknowledgement

We thank Dr. A. Neels from the Crystallographic Service of the University of Neuchâtel for solving the crystal structures.

Appendix A. Supplementary data

Supplementary data associated with this article can be found, in the online version, at doi:10.1016/j.jfluchem.2011.11.009.

References

[1] K. Merz, V. Vasylyeva, CrystEngComm 12 (2010) 3989–4002.
[2] (a) A. Schwarzer, P. Bombicz, E. Weber, J. Fluorine Chem. 131 (2010) 345–356; (b) A. Schwarzer, E. Weber, Cryst. Growth Des. 8 (2008) 2862–2874.
[3] E.R.T. Tiekink, J.J. Vittal, M.J. Zaworotko (Eds.), Organic Crystal Engineering, Wiley, Chichester, 2010.
[4] C.B. Aakeröy, N.R. Champness, C. Janiak, CrystEngComm 12 (2010) 22–43.
[5] H. Klauk (Ed.), Organic Electronics, Wiley-VCH, Weinheim, 2006.
[6] T.J.J. Müller, U.H.F. Bunz (Eds.), Functional Organic Materials, Wiley-VCH, Weinheim, 2007.
[7] J. Bernstein, Polymorphism in Molecular Crystals, Clarendon, Oxford, 2002.
[8] P.A. Wright, Microporous Framework Solids, Royal Society of Chemistry, Cambridge, 2008.
[9] (a) G.R. Desiraju, Acc. Chem. Res. 35 (2002) 565–573;
(b) G.R. Desiraju, T. Steiner, The Weak Hydrogen Bond in Chemistry and Biology, Oxford University Press, Oxford, 1999.
[10] M. Nishio, Y. Umezawa, K. Honda, S. Tsuboyama, H. Suezawa, CrystEngComm 11 (2009) 1757–1788.

[11] (a) S.L. James, in: J.L. Atwood, J.M. Steed (Eds.), Encyclopedia of Supramolecular Chemistry, Dekker, New York, 2004, pp. 1093–1099;
(b) C. Janiak, J. Chem. Soc. Dalton Trans. (2000) 3885–3896.

[12] (a) G.R. Desiraju, Angew. Chem. Int. Ed. 34 (1995) 2311–2327;
(b) A. Nangia, G.R. Desiraju, in: E. Weber (Ed.), Topics in Current Chemistry, vol. 198, Springer, Berlin/Heidelberg, 1998.

[13] (a) P. Metrangolo, G. Resnati, T. Pilati, S. Biella, in: P. Metrangolo, G. Resnati (Eds.), Structure and Bonding, vol. 126, Springer, Berlin/Heidelberg, 2008, pp. 105–136;
(b) M. Fourmigué, Curr. Opin. Solid State Mater. Sci. 13 (2009) 36–45.

[14] (a) R. Fröhlich, T.C. Rosen, O.G.J. Meyer, K. Rissanen, G. Haufe, J. Mol. Struct. 787 (2006) 50–62;
(b) V. Vasylyeva, K. Merz, Cryst. Growth Des. 10 (2010) 2550–2555;
(c) A.G. Dikundwar, C. Venkateswarlu, R.O. Piltz, S. Chandrasekaran, T.N. Guru Row, CrystEngComm 13 (2011) 1531–1538;
(d) H.Y. Lee, A. Olasz, M. Pink, H. Park, D. Lee, Chem. Commun. 47 (2011) 481–483.

[15] (a) K. Reichenbächer, H.I. Süss, J. Hulliger, Chem. Soc. Rev. 34 (2005) 22–30;
(b) R. Berger, G. Resnati, P. Metrangolo, E. Weber, J. Hulliger, Chem. Soc. Rev. 40 (2011) 3496–3508.

[16] P. Kirsch, Modern Fluoroorganic Chemistry, Wiley-VCH, Weinheim, 2004.

[17] T.M. Fasina, J.C. Collings, D.P. Lydon, D. Albesa-Jové, A.S. Batsanov, J.A.K. Howard, P. Nguyen, M. Bruce, A.J. Scott, W. Clegg, S.W. Watt, C. Viney, T.B. Marder, J. Mater. Chem. 14 (2004) 2395–2404.

[18] T.M. Fasina, J.C. Collings, J.M. Burke, A.S. Batsanov, R.M. Ward, D. Albesa-Jové, L. Porrès, A. Beeby, J.A.K. Howard, A.J. Scott, W. Clegg, S.W. Watt, C. Viney, T.B. Marder, J. Mater. Chem. 15 (2005) 690–697.

[19] R. Mariaca, G. Labat, N.-R. Behrnd, M. Bonin, F. Helbling, P. Eggli, G. Couderc, A. Neels, H. Stoeckli-Evans, J. Hulliger, J. Fluorine Chem. 130 (2009) 175–196.

[20] J.C. Collings, J.M. Burke, P.S. Smith, A.S. Batsanov, J.A.K. Howard, T.B. Marder, Org. Biomol. Chem 2 (2004) 3172–3178.

[21] T. Shirman, J.-F. Lamera, L.J.W. Shimon, T. Gupta, J.M.L. Martin, M.E. van der Boom, Cryst. Growth Des. 8 (2008) 3066–3072.

[22] R. Chinchilla, C. Najera, Chem. Rev. 107 (2007) 874–922.

[23] A. Bondi, J. Phys. Chem. 68 (1964) 441–451.

[24] (a) S.E. Wheeler, K.N. Houk, J. Am. Chem. Soc. 130 (2008) 10854–10855;
(b) S.E. Wheeler, K.N. Houk, J. Chem. Theory Comput. 5 (2009) 2301–2312;
(c) S.E. Wheeler, A.J. McNeil, P. Müller, T.M. Swager, K.N. Houk, J. Am. Chem. Soc. 132 (2010) 3304–3311;
(d) S.E. Wheeler, J. Am. Chem. Soc. 133 (2011) 10262–10274.

[25] J. Potenza, D. Mastropaolo, Acta Crystallogr. B 31 (1975) 2527–2529.

[26] (a) J.C. Collings, K.P. Roscoe, E.G. Robins, A.S. Batsanov, L.M. Stimson, J.A.K. Howard, T.B. Marder, New J. Chem. 25 (2001) 1410–1417;
(b) J.C. Collings, K.P. Roscoe, E.G. Robins, A.S. Batsanov, L.M. Stimson, J.A.K. Howard, S.J. Clark, T.B. Marder, New J. Chem. 26 (2002) 1740–1746.

[27] E.A. Meyer, R.K. Castellano, F. Diederich, Angew. Chem. Int. Ed. 42 (2003) 1210–1250.

[28] C.A. Hunter, K.R. Lawson, J. Perkins, C.J. Urch, J. Chem. Soc. Perkin Trans. 2 (2001) 651–669.

[29] (a) J.D. Dunitz, Chembiochem 5 (2004) 614–621;
(b) L.M. See also:, M. Salonen, F. Ellermann, Diederich, Angew. Chem. Int. Ed. 50 (2011) 4808–4842.

[30] M.S. Sivaramkumar, R. Velmurugan, M. Sekar, P. Ramesh, M.N. Ponnuswamy, Acta Crystallogr. E 66 (2010) o1820.

[31] N.I. Golovina, A.N. Titkov, A.V. Raevskii, L.O. Atovmyan, J. Solid State Chem. 113 (1994) 229–238.

[32] (a) P. Metrangolo, J.S. Murray, T. Pilati, P. Politzer, G. Resnati, Cryst. Growth Des. 11 (2011) 4238–4246;
(b) P. Metrangolo, J.S. Murray, T. Pilati, P. Politzer, G. Resnati, G. Terraneo, CrystEngComm 13 (2011) 6593–6596.

[33] M. Colapietro, A. Domenicano, C. Marciante, G. Portalone, Z. Naturforsch. 37B (1982) 1309–1311.

[34] E.M. Graham, V.M. Miskowski, J.W. Perry, D.R. Coulter, A.E. Stiegman, W.P. Schaefer, R.E. Marsh, J. Am. Chem. Soc. 111 (1989) 8771–8778.

[35] P. Metrangolo, F. Meyer, T. Pilati, G. Resnati, G. Terranneo, Angew. Chem. Int. Ed. 47 (2008) 6114–6127.

[36] R. Thomas, S. Lakshmi, S.K. Pati, G.U. Kulkarni, J. Phys. Chem. B 110 (2006) 24674–24677.

[37] C.E. Smith, P.S. Smith, R.L. Thomas, E.G. Robins, J.C. Collings, C. Dai, A.J. Scott, S. Borwick, A.S. Batsanov, S.W. Watt, S.J. Clark, C. Viney, J.A.K. Howard, W. Clegg, T.B. Marder, J. Mater. Chem. 14 (2004) 413–420.

[38] G. Marras, P. Metrangolo, F. Meyer, T. Pilati, G. Resnati, A. Vij, New J. Chem. 30 (2006) 1397–1402.

[39] M. Hesse, H. Meier, B. Zeeh, Spektroskopische Methoden in der Organischen Chemie, Thieme, Stuttgart/New York, 2002.

[40] J.M. Birchall, R.N. Haszeldine, H.E. Jones, J. Chem. Soc. C (1971) 1343–1348.

[41] F. Naso, L. Ronzini, J. Chem. Soc. Perkin Trans. 1 (1974) 340–343.

[42] K.A. Leonhard, J.P. Hall, M.I. Nelen, S.R. Davies, S.O. Gollnick, S. Camacho, A.R. Oseroff, S.L. Gibbson, R. Hilf, M.R. Detty, J. Med. Chem. 43 (2000) 4488–4498.

[43] Y. Zhang, J. Wen, J. Chem. Res. Synop. (1991) 20–21.

[44] G.M. Sheldrick, SHELXS-97. Program for Crystal Structure Solution, University of Göttingen, Göttingen, Germany, 2008.

[45] G.M. Sheldrick, SHELXL-97. Program for Crystal Structure Refinement, University of Göttingen, Göttingen, Germany, 2008.